Chapter 2

Miniature Planar Antenna Design for Ultra-Wideband Systems

Mohammad Alibakhshikenari, Mohammad Naser-Moghadasi, Ramazan Ali Sadeghzadeh, Bal Singh Virdee and Ernesto Limiti

Additional information is available at the end of the chapter

http://dx.doi.org/10.5772/intechopen.68612

Abstract

Demand for antennas that are compact and operate over an ultra-wideband (UWB) frequency range is growing rapidly as UWB systems offer high resolution imaging capability and high data rate transmission in the order of Gb/s that is required by the next generation of wireless communication systems. Hence, over the recent years the research and development of UWB antennas has been widely reported in literature. The main performance requirements sought from such antennas include: (1) low VSWR of <2; (2) operation over 7.6 GHz from 3 to 10.6 GHz; and (3) good overall radiation characteristics. Significant size reduction and low manufacturing cost are also important criteria in order to realize a cost-effective and miniature system. Other desirable requirements include compatibility and ease of integration with RF electronics.

Keywords: ultra-wideband antenna, metamaterial, composite right/left-handed transmission line, antenna miniaturization, slit antennas

1. Introduction

Ever since the Federal Communications Commission (FCC) released a bandwidth of 7.5 GHz (from 3.1 to 10.6 GHz) for ultra-wideband (UWB) wireless communications, UWB technology has rapidly developed for high data rate wireless communications [1–5]. As is the case in conventional narrowband wireless communication systems, an antenna plays a very crucial role in UWB systems. However, there are greater challenges in designing a UWB antenna than a narrow band one. A suitable UWB antenna should be capable of operating over an ultra-wide

bandwidth as defined by the FCC. At the same time, satisfactory radiation properties over the UWB frequency range are also necessary, including nondispersive nature in order to minimize distortion in the transmitted signal. The antenna needs to have a low voltage standing wave ratio (VSWR) (<2) over 3.1–10.6 GHz band and omnidirectional radiation characteristics [6]. Nowadays, in most applications significant size reduction of antennas is paramount in order to achieve minimization of communication systems. Other desirable features include being a planar structure that is cost-effective to fabricate in large volumes.

Design of a UWB antennas is challenging for systems operating at the lower part of the microwave spectrum. This is due to the fact that the wavelength is very large at these frequencies and the resulting physically large antennas are not desirable due to space limitations of modern systems. This problem is particularly severe in systems that operate at HF, VHF, and UHF bands. This is because in such applications having antennas with low visual signatures is of paramount importance. The current antennas of choice for these applications tend to be monopole whip antennas. These antennas, however, suffer from two major drawbacks. First, the relatively large heights of a conventional monopole whip antenna, when mounted on a vehicle, such an antenna significantly protrudes from the top surface of the vehicle drastically increasing the visual signature of the vehicle. The second issue with monopole whip antennas is their narrow bandwidths, which limits the types of waveforms that they can receive or transmit. Therefore, development of compact, low-profile, and ultra-wideband antennas is of particular interest in many communications systems that operate at HF, VHF, and UHF frequencies. To increase the bandwidth of monopole-type radiators, a number of different techniques have been examined. A variety of printed monopole antennas that provide UWB operation in a planar form factor are examined in the 3.1–10.6 GHz band [7–9]. However, at its lowest frequency of operation, a printed monopole tends to have relatively large dimensions.

Numerous techniques have been investigated and reported in recent years to reduce the size of microstrip antennas. These techniques are mainly based on loading a patch antenna with reactive components realized with suitably designed slots, shorting posts, and lumped elements. The effectiveness of these techniques is, however, limited in the reduction of the footprint of planar antennas which is required by modern wireless systems [10–12]. The size of patch antennas can also be reduced by fabricating the antenna on dielectric substrates with a high permittivity. This well-established technique, however, results in increased surface wave excitation over the antenna that degrades its impedance bandwidth, radiation efficiency, and its radiation characteristics [13].

Techniques mentioned above fail to meet the challenges for miniaturization of antennas. In this chapter, the exploitation of artificially engineered materials that are based on metamaterial transmission lines is shown to provide the solution for miniaturization of planar antennas [14–22]. In fact metamaterials, which are also accurately referred to as composite right-/left-handed (CRLH) transmission lines, are a novel paradigm in electromagnetic engineering as such materials exhibit electrical characteristics, that is, negative permittivity and permeability, not possible with naturally occurring materials [11]. These properties are exploited in this chapter to design planar antennas with a small footprint using standard manufacturing photolithography techniques [11–18]. In particular, in this chapter, a unique CRLH-TL structure is employed in the design of an antenna using conventional microwave integrated

circuit (MIC) manufacturing techniques. The unit cells of the CRLH-TL structure was realized by engraving L- and T-shaped slits on a rectangular conductor that is grounded through a high impedance microstrip stub that are spiraled. In the antenna the L- and T-shaped slits exhibit capacitive property, and the stub acts like an inductor. The antenna structure, which was created using these unit cells, was modeled and optimized for UWB performance while maintaining its radiation characteristics in terms of gain and radiation efficiency.

2. Composite right-/left-handed antenna design

A left-handed transmission line structure can be created from an arrangement consisting of a series capacitor and shunt inductor. This *LC* circuit configuration can be achieved for antenna applications by simply etching a dielectric slot in a metallic-radiating patch, where the patch is grounded using a high impedance microstrip line. The slot created in the patch acts like a series capacitance C_L and the high impedance microstrip line acts like a shunt inductance L_L. The inductive element in the structure can be coiled to reduce the overall footprint of the antenna structure [23, 24]. This approach is used here to implement a compact antenna by cascading together a number of CRLH transmission line unit cells comprising left-handed *LC* unit cells.

The equivalent circuit model for a lossless CRLH transmission line unit cell is shown in **Figure 1**. It consists of a per-unit length impedance Z (W/m) constituted by a right-handed per-unit-length inductance L_R (H/m) in series with a left-handed per-unit-length capacitance C_L (F/m), and a per-unit-length admittance Y (S/m) constituted by a right-handed per-unit-length capacitance C_R (F/m) in parallel with a left-handed per-unit-length inductance L_L (H/m). The complex propagation constant γ and the propagation constant β of the CRLH transmission line unit cell are given by

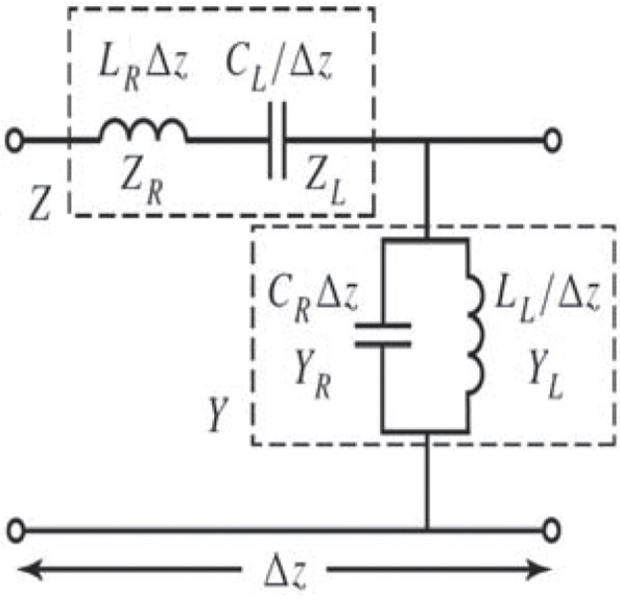

Figure 1. Equivalent circuit model for an ideal CRLH transmission line.

$$\gamma = \alpha + j\beta = \sqrt{ZY} \tag{1}$$

Where

$$\beta(\omega) = s(\omega)\sqrt{\omega^2 L_R C_R + \frac{1}{\omega^2 L_L C_L} - \left(\frac{L_R}{L_L} + \frac{C_R}{C_L}\right)} \tag{2}$$

$$s(\omega) = \begin{Bmatrix} -1 \; if \omega < \omega_{se} = \min\left(\frac{1}{\sqrt{L_R C_L}}, \frac{1}{\sqrt{L_L C_R}}\right) \\ 0 \; if \; \omega_{se} < \omega < \omega_{sh} \\ +1 \; if \omega > \omega_{sh} = \max\left(\frac{1}{\sqrt{L_R C_L}}, \frac{1}{\sqrt{L_L C_R}}\right) \end{Bmatrix} \tag{3}$$

and

$$Z(\omega) = j\left(\omega L_R - \frac{1}{\omega C_L}\right) \tag{4}$$

$$Y(\omega) = j\left(\omega C_R - \frac{1}{\omega L_L}\right) \tag{5}$$

where $\beta(\omega)$, $s(\omega)$, $Z(\omega)$, and $Y(\omega)$ represent the dispersion relation, sign function, impedance, and admittance of the antenna structure, respectively. Series and shunt resonance frequencies, respectively, are given by

$$\omega_{se} = \frac{1}{\sqrt{L_R C_L}} \tag{6}$$

$$\omega_{sh} = \frac{1}{\sqrt{L_L C_R}} \tag{7}$$

The unit cell's permittivity and permeability are given by

$$\mu = \frac{Z}{j\omega} = L_R - \frac{1}{\omega^2 C_L} \tag{8}$$

$$\varepsilon = \frac{Y}{j\omega} = C_R - \frac{1}{\omega^2 L_L} \tag{9}$$

The prototype antenna based on CRLH transmission line unit cells, shown in **Figure 2**, consists of L- and T-shaped slits etched on a rectangular radiation patch. The patch is short-circuited to ground through high impedance microstrip lines that are coiled to reduce the antennas' size. Appropriate number of CRLH unit cells is cascaded together in the antenna that is terminated in a matched load to achieve the required bandwidth and radiation characteristics. The antenna was fabricated on glass-reinforced epoxy FR-4 substrate with a dielectric constant of 4.6, thickness of 0.8 mm, and loss tangent of 1×10^{-3}. Standard manufacturing technique was used to realize the antenna.

The antenna design was first analyzed and optimized using ANSYS high frequency structure simulator (HFSS™). Two waveguide ports were defined to represent the input and output of the antenna structure, as shown in **Figure 2(a)**, in order to evaluate its performance. The antenna was excited at port 1 through an SMA connector, and terminated to a matched 50 Ω load at port 2 using surface mount technology (SMD1206) of dimensions 3.5×1.8 mm^2.

http://dx.doi.org/10.5772/intechopen.68612

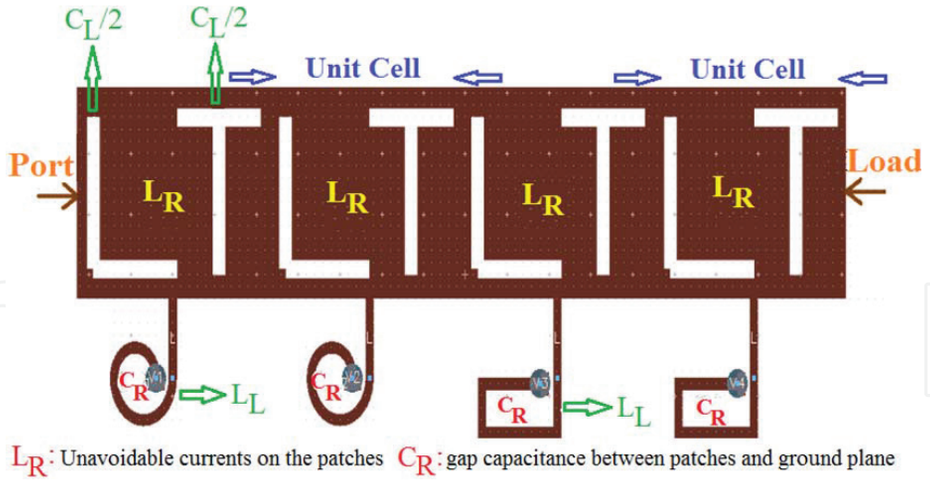

(a)

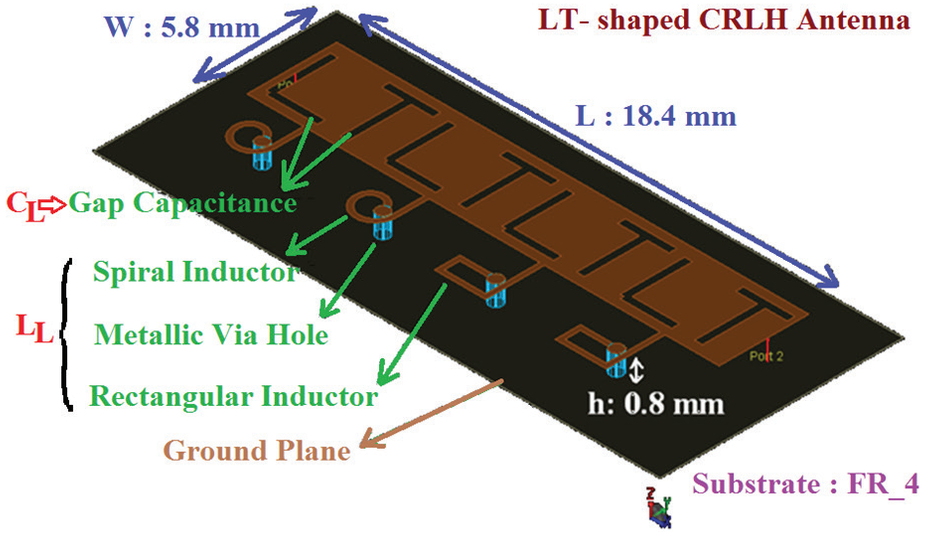

(b)

(c)

Figure 2. The proposed antenna based on four CRLH transmission line unit cells. (a) Configuartion of the proposed CRLH transmission line antenna. (b) Isometric view of the proposed CRLH transmission line antenna. (c) Fabricated antenna prototype.

A more accurate model of the proposed CRLH transmission line unit cell that is employed in the antenna is shown in **Figure 3**. The model includes loss components in the unit cell structure that are represented by right-handed resistance (R_R) and conductance (G_R), and left-handed resistance (R_L) and conductance (G_L). These parameters account for the radiation emitted by the antenna. Optimized magnitudes of these parameters in the unit cell were obtained from ANSYS HFSS™, that is, L_L = 6 nH, C_L = 2.4 pF, L_R = 2 nH, C_R = 1 pF, R_L = 5 Ω, R_R = 3 Ω, G_L = 4.5 ʊ, and G_R = 2 ʊ.

The actual antenna's dimensions are 22.6 × 5.8 × 0.8 mm^3 or 0.037 λ_0 × 0.009 λ_0 × 0.001 λ_0, where λ_0 is free space wavelength at 0.5 GHz. The simulated and measured impedance bandwidth of the antenna are 11.1 GHz (0.35–11.45 GHz) and 10.8 GHz (0.5–11.3 GHz), respectively, for voltage standing wave ratio (VSWR) < 2. This corresponds to a fractional bandwidth of 188% for the simulation result, and 183% for the measured result. The reflection coefficients and the measured VSWR of the proposed miniaturized antenna are shown in **Figure 4**. The simulated and measured group delay response depicted in **Figure 5** shows the group delay variation is under 0.25 ns for a large frequency range up to 16 GHz.

Results of the parametric study are shown in **Figure 6**. It is evident from these results that the antenna's gain and radiation efficiency can be improved by increasing the number of CRLH unit cells. The peak gain and radiation efficiency are obtained at around 8 GHz. Gain of greater than 4 dBi from 2.9–12.6 GHz is achieved for a unit cell of four. Over this frequency range, the radiation efficiency exceeds 50%. As the proposed antenna had to fit within an area of 23 × 6 mm^2, the number of unit cells selected in the design was therefore four.

The simulated and measured gain and radiation efficiency of the antenna at various frequencies are given in **Tables 1** and **2**. The results in these tables show a better performance obtained from the antenna over higher frequencies than at the lower frequencies. The simulated three-dimensional (3-D) and measured two-dimensional (2-D) radiation patterns of the compact CRLH antenna at various frequencies are shown in **Figures 7** and **8**, respectively. The results show the cross-polarization is comparable or higher than copolarization at certain frequencies, however, over a small angular range in both the E- and H-planes. This is observed in

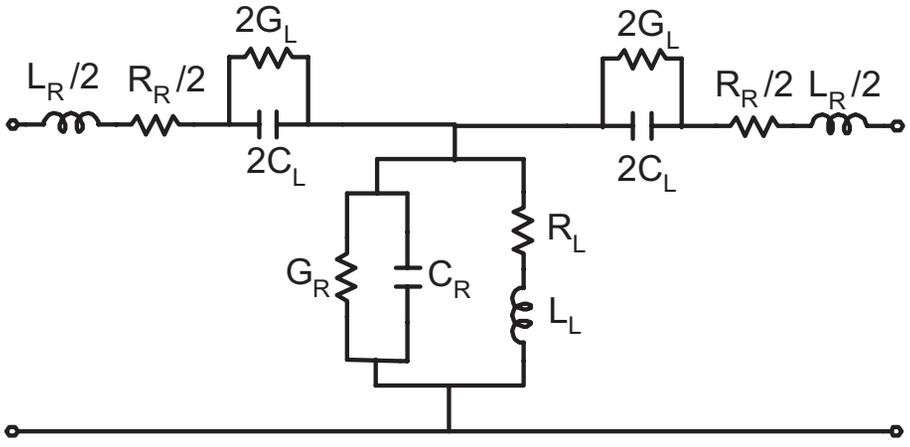

Figure 3. Equivalent circuit model of the CRLH unit cell employed in the proposed antenna.

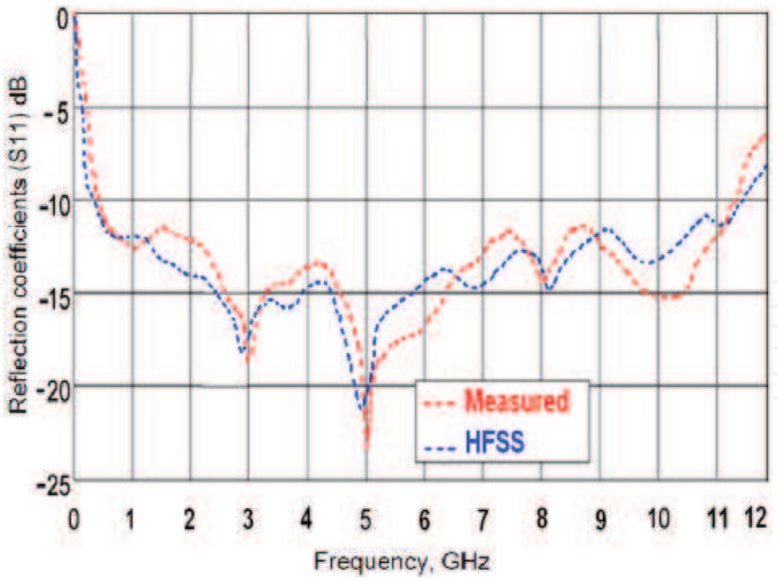

(a)

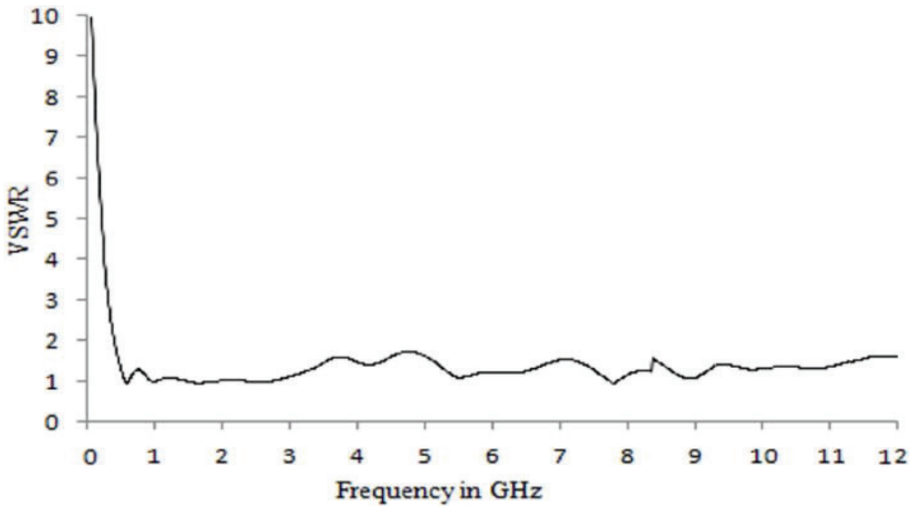

(b)

Figure 4. Reflection coefficient and measured VSWR response of the CRLH transmission line antenna. (a) Simulated and measured reflection coefficient response. (b) Antenna's measured VSWR response.

other CRLH antennas too [25–31] which present scope for improvement of such antennas. Cross-polarization can be reduced by loading the shorting pins, which has been demonstrated for patch antennas [32–35]. The shorting pins are located in the centerline of a square patch to strengthen the surface current density near the feeding point at edge. Because of symmetric arrangement of these two shorting pins, surface current density on the patch is maintained as the odd-symmetric property with respect to the H-plane, thus tremendously degrading the cross-polarization level. Such a solution is worthy of investigation in CRLH antennas.

The measured gain and radiation efficiency of the CRLH antenna is shown in **Figure 9**. The antenna has a peak gain of 6.5 dBi and radiation efficiency of 88% at around 8 GHz. The antenna has a gain that exceeds 4 dBi over 3.5–12.5 GHz, and radiation efficiency over this frequency range is greater than 53%.

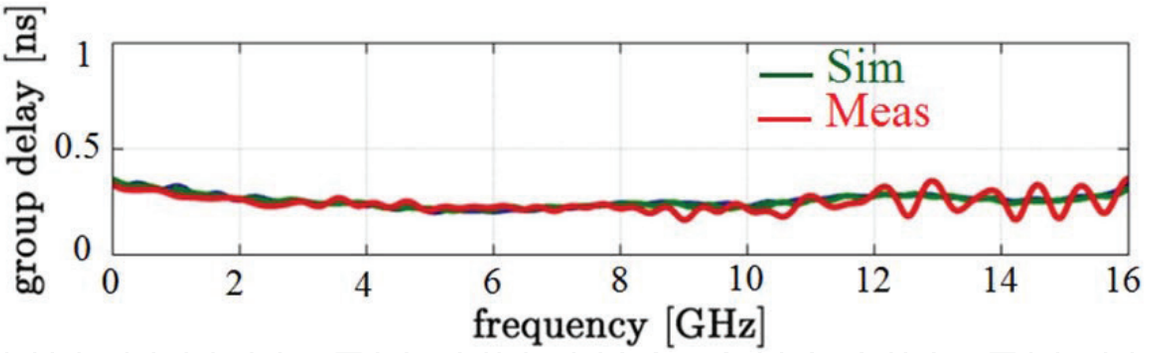

Figure 5. Group delay response of the CRLH transmission line antenna.

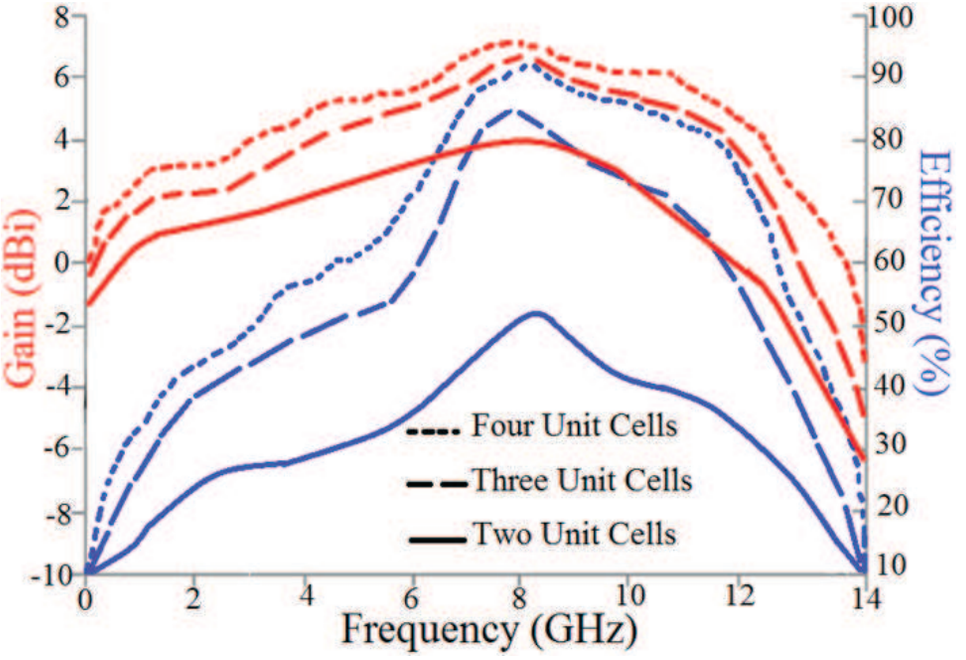

Figure 6. The antenna's simulated radiation gain and efficiency response as a function of number of unit cells.

Frequency (GHz)	0.5	3	5	8	11.3
Gain (dBi)	1.7	3.8	5.1	7	6.1
Efficiency (%)	25	50	62	91	79

Table 1. Simulated gain and radiation efficiency.

Table 3 shows the proposed antenna's salient features. The antenna is highly compact and operates over an ultra-wideband (UWB). In addition, it can be easily integrated with RF circuits making it suitable for UWB wireless communication systems. Characteristics of the CRLH antenna are compared with other recently reported antennas in **Table 4**.

Frequency (GHz)	0.5	3	5	8	11.3
Gain (dBi)	1.5	3.4	4.8	6.5	5.7
Efficiency (%)	20	45	57	88	73

Table 2. Measured gain and radiation efficiency.

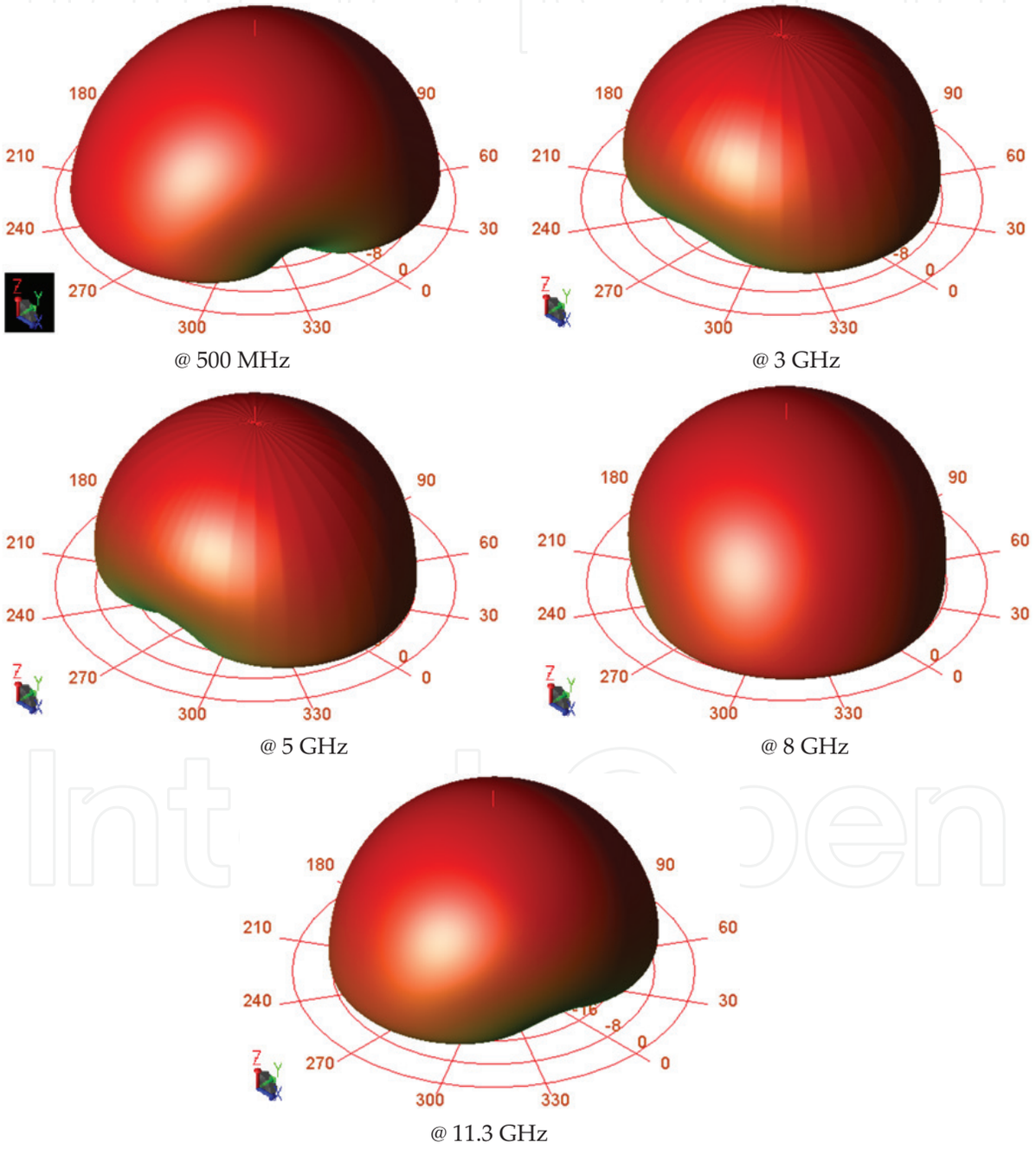

Figure 7. Simulated 3-D radiation patterns of the CRLH antenna.

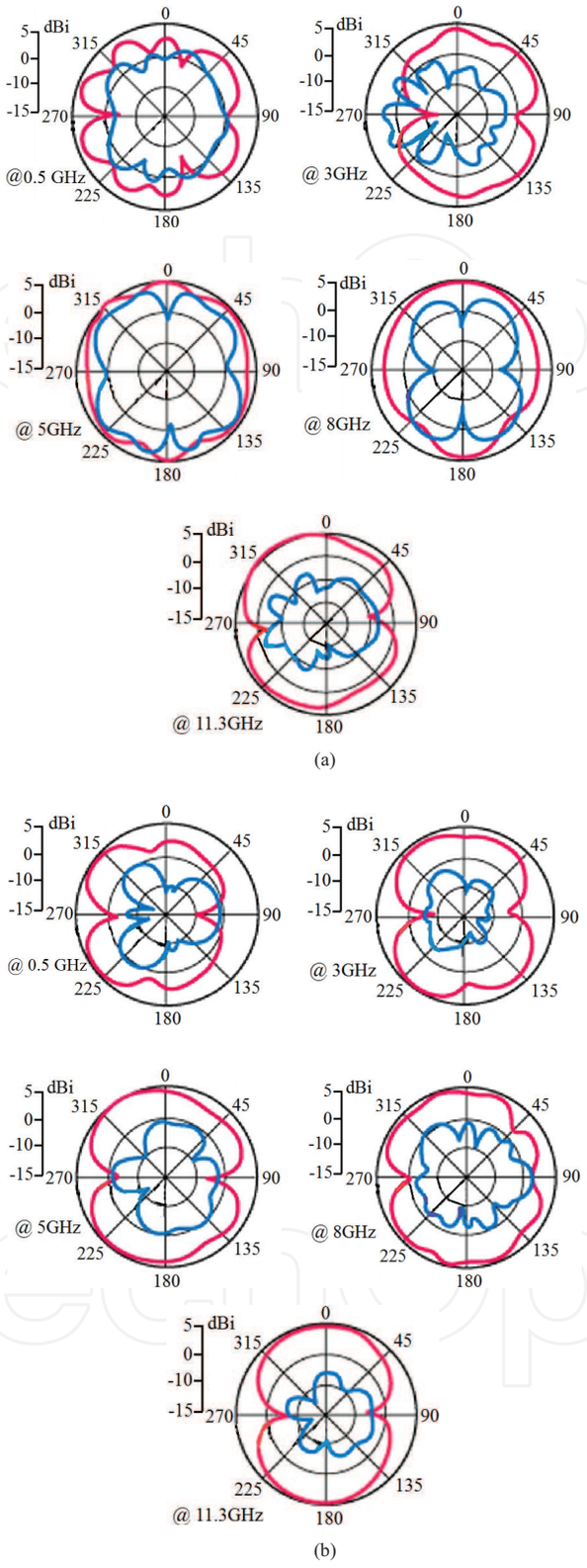

Figure 8. The measured radiation patterns of the CRLH transmission line antenna in the E- and H-planes. (a) Measured E-plane co and cross radiation patterns (Co: red line, Cross: blue line). (b) Measured H-plane co and cross radiation patterns (Co: red line, Cross: blue line).

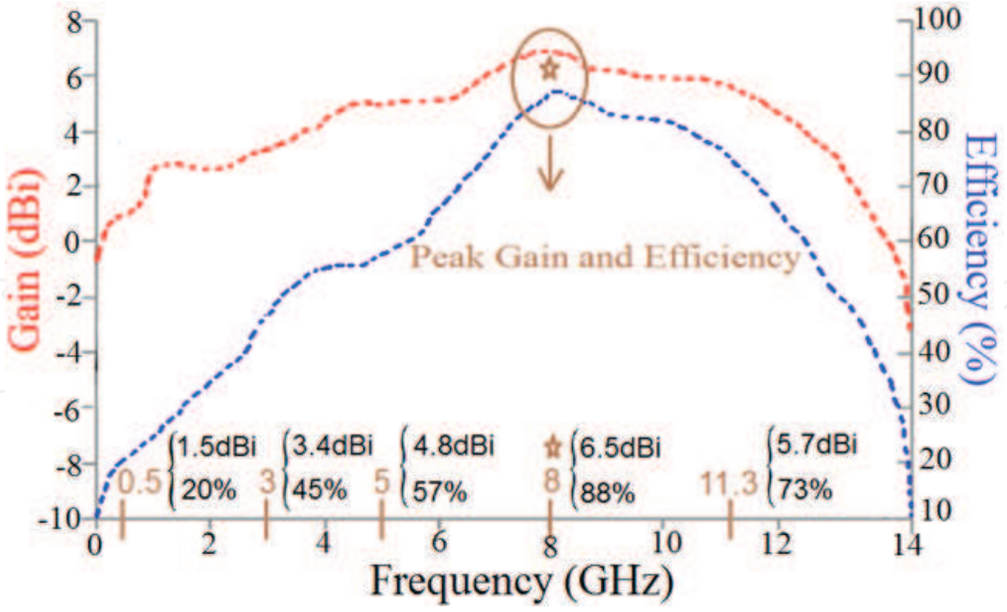

Figure 9. Measured gain and radiation efficiency response of the CRLH antenna.

Dimensions	22.6 × 5.8 × 0.8 mm^3
	0.037 λ_0 × 0.009 λ_0 × 0.001 λ_0 at 0.5 GHz
Bandwidth	10.8 GHz (500 MHz–11.3 GHz)
	(Fractional bandwidth = 183%)
Gain (dBi)	6.5 (max) at 8 GHz
	≥4 from 2.9–12.6 GHz
Efficiency (%)	88 (max) at 8 GHz
	≥50% from 2.9–12.6 GHz

Table 3. Measured characteristics of the CRLH antenna.

Reference	Dimensions	Fractional bandwidth (%)	Peak gain (dBi)	Max. efficiency (%)
[2]	0.051 λ_0 × 0.016 λ_0 × 0.002 λ_0	123.8	2.8	70
[6] with 7 unit cells	0.556 λ_0 × 0.179 λ_0 × 0.041 λ_0	87.16	3.4	68.1
[6] with 8 unit cells	0.564 λ_0 × 0.175 λ_0 × 0.02 λ_0	84.23	2.35	48.2
[23]	0.047 λ_0 × 0.021λ_0 × 0.002 λ_0	104.76	2.3	62
Proposed antenna	0.037 λ_0 × 0.009 λ_0 × 0.001 λ_0	183	6.5	88

Table 4. Comparison of the CRLH antenna with other reported antennas.

To summarize, this chapter presented the design and measured results of a novel antenna that is based on CRLH transmission lines. The antenna is highly compact planar structure with dimensions of 22.6 × 5.8 × 0.8 mm^3 and possesses desirable characteristics of ultra-wideband performance (500 MHz–11.3 GHz) with gain and radiation efficiency of 6.5 dBi and 88%, respectively, at 8 GHz. The low cost antenna is simple to design and easy to fabricate using standard manufacturing techniques. The CRLH transmission line unit cell constituting the antenna is realized by etching L- and T-shaped dielectric slots inside a rectangular patch, which is grounded through a high impedance transmission line. By cascading together several unit cells, the desired bandwidth and radiation characteristics can be obtained. In addition, the antenna can be easily integrated with RF electronics.

Author details

Mohammad Alibakhshikenari[1]*, Mohammad Naser-Moghadasi[2], Ramazan Ali Sadeghzadeh[3], Bal Singh Virdee[4] and Ernesto Limiti[1]

*Address all correspondence to: alibakhshikenari@ing.uniroma2.it

1 Electronic Engineering Department, University of Rome "Tor Vergata", Rome, Italy

2 Faculty of Engineering, Science and Research Branch, Islamic Azad University, Tehran, Iran

3 Faculty of Electrical Engineering, K. N. Toosi University of Technology, Tehran, Iran

4 London Metropolitan University, Center for Communications Technology, London, UK

References

[1] Alibakhshi Kenari M. Design and modelling of New UWB metamaterial planar cavity antennas with shrinking of the physical size for modern transceivers. International Journal of Antennas and Propagation. 2013; **2013**:12. Article ID 56253. DOI: 10.1155/2013/562538.

[2] Anon., FCC First Report and Order on Ultra Wideband Technology, Feb. 2002.

[3] Wang YJ, Lee CK, Tian PS, Lee SW. "Novel microstrip-monopole integrated ultra wideband antenna for mobile UWB devices", Radio and Wireless Conference, 2003. RAWCON '03. Proceedings, pp. 87-90, 10-13 August 2003.

[4] Taniguchi T, Kobayashi T. An Omnidirectional and low-VSWR antenna for the FCC-approved UWB frequency band. IEEE International Symposium on Antennas and Propagation. 2003;**13**:460-463

[5] Sorgel W, Waldschmidt C, Wiesbeck W. Transient response of a vivaldi antenna and a logarithmic periodic dipole array for ultra wideband communication. IEEE International Symposium on Antennas and Propagation. 2003;**3**:592-595

[6] Alibakhshi-Kenari M, Naser-Moghadasi M, and Sadeghzadeh RA. Composite right-/left-handed-based antenna with wide applications in very-high frequency/ultra-high

frequency bands for radio transceivers. IET Microwaves, Antennas & Propagation. 2015;**9**(15):1713 –1726.

[7] Liang J, Chiau CC, Chen X, Parini CG. Study of a printed circular disc monopole antenna for UWB systems. IEEE Transactions of Antennas Propagation. 2005;**53**(11):3500-3504

[8] Chen ZN, See TSP, Qing X. Small printed ultrawideband antenna with reduced ground plane effect. IEEE Transactions of Antennas Propagation. 2007;**55**(2):383-388

[9] Dissanayake T, Esselle KP. Prediction of the notch frequency of slot loaded printed UWB antennas. IEEE Transactions of Antennas Propagation. 2007;**55**(11):3320-3325

[10] Wheeler HA. Fundamental limitations of small antennas. Proceedings of IRE.1947; **35**:1479-1484

[11] Caloz C, Itoh CT. Electromagnetic Metamaterials Transmission Line Theory and Microwave Applications, New Jersey: John Wiley & Sons, Inc.; 2006

[12] Porath R. Theory of miniaturized shorting-post microstrip antennas. IEEE Transactions of Antennas Propagation. 2000;**48**(1):41-47

[13] Stutzman WL. Antenna Theory and Design. J. Wiley & Sons.; 1997

[14] Balanis CA. Antenna Theory and Design. John Wiley & Sons.; 2016

[15] Jahani S, Rashed-Mohassel J, Shahabadi M. Miniaturization of circular patch antennas using MNG metamaterials. IEEE Antennas and Wireless Propagation Letters. 2010;**9**:1194-1196

[16] Wang C, Hu BJ, Zhang XY. Compact triband patch antenna with large scale of frequency ration using CRLH-TL structures. IEEE Antennas and Wireless Propagation Letters. 2010;**9**:744-746

[17] Bilotti F, Alu A, Vegni L. Design of miniaturized metamaterial patch antennas with μ-negative loading. IEEE Transaction on Antennas and Propagation. 2008;**56**(6):814-818

[18] Engheta N, Ziolkowski RW. Metamaterials: Physics and Engineering Explorations. New York: Wiley; 2006

[19] Eleftheriades GV, Balmain KG. Negative Refraction Metamaterials: Fundamental Principles and Applications. New York: John Wiley & Sons; 2005

[20] Slyusar VI. "Metamaterials on antenna solutions", International Conference on Antenna Theory and Techniques (ICATT). 2009.

[21] Lee CJ, Leong K, Itoh T. Composite right/left-handed transmission line based compact resonant antennas for RF module integration. IEEE Transactions of Antennas and Propagation. 2006;**54**(8):2283-2291

[22] Lee CJ, Huang W, Gummalla A, Achour M. Small antennas based on CRLH structures: Concept, design, and applications. IEEE Antennas and Propagation Magazine. 2011;**53**(2):10-25

[23] Alibakhshi Kenari M. Printed planar patch antennas based on metamaterial. International Journal of Electronics Letters. 2014;**2**(1):37-42. http://dx.doi.org/10.1080/21681724.2013.874042

[24] Alibakhshi-Kenari M, Movahhedi M, Naderian H. A new miniature ultra wide band planar microstrip antenna based on the metamaterial transmission line. IEEE Asia-Pacific Conference on Applied Electromagnetics (APCAE), Dec. 2012, pp. 293-297, Malaysia.

[25] Zheng L, Quan XL, Liu HJ, Li RL. Broadband planar antenna based on CRLH structure for DVB-H and GSM-900 applications. Electronics Letters. 2012;**48**(23):1443-1444

[26] Wu GC, Wang GM, Peng HX, Gao XJ, Liang JG. Design of leaky-wave antenna with wide beam-scanning angle and low cross polarisation using novel miniaturised composite right/left-handed transmission line. IET Microwave Antennas Propagation. 2016;**10**(7):777-783

[27] Nandi S, Mohan A. A miniaturized dual mode CRLH unit cell loaded SIW antenna. 5th IEEE Applied Electromagnetics Conference (AEMC) 2015, 18th- 21st, December 2015, pp. 1-2.

[28] Lee H, Woo DJ, Nam S. Compact and bandwidth-enhanced asymmetric coplanar waveguide (ACPW) antenna using CRLH-TL and modified ground plane. IEEE Antennas and Wireless Propagation Letters. 2016;**15**:810-813

[29] Saurav K, Sarkar D, Srivastava KV. CRLH unit-cell loaded multiband printed dipole antenna. IEEE Antennas and Wireless Propagation Letters. 2014;**13**:852-855

[30] Yan S, Soh PJ, Vandenbosch GAE. Wearable dual-band composite right/left-handed waveguide textile antenna for WLAN applications. Electronics Letters. 2014;**50**(6):424-426

[31] Xu HX, Wang GM, Qi MQ, Cai T. Compact fractal left-handed structures for improved cross-polarization radiation pattern. IEEE Transactions on Antennas and Propagation. 2014;**62**(2):546-554

[32] Zhang X, Zhu L. Patch antennas with loading of a pair of shorting pins toward flexible impedance matching and low cross polarization. IEEE Transactions on Antennas and Propagation. 2016;**64**(4):1226-1233

[33] Ghosh D, et al. Physical and quatitative analysis of compact rectangular microstrip antenna with shorted non radiating edges for reduced cross polarized radiation using modified cavity model. IEEE Antennas & Propagations Magazine. 2014;**56**(4):61-72.

[34] Ghosh A, et al. Rectangular microstrip antenna on slot-type defected ground for reduced cross-polarized radiation. IEEE Antennas and Wireless Propagation Letters. 2015;**14**:321-324

[35] Chakraborty S, et al. Substrate fields modulation with defected ground structure: A key to realize high gain, wideband microstrip antenna with improved polarization purity in principal and diagonal planes. International Journal of RF and Microwave Computer Aided Engineering, (Wiley). 2016;**26**(2):174-181